2023 IEEE/ASME International Conference on Advanced Intelligent Mechatronics (AIM)
June 28-30, 2023. Seattle, Washington, USA

A Hybrid Impedance and Admittance Control Strategy for a Shape-Transformable Leg-Wheel

Yuan-Cheng Zhuang, Yu-Ju Liu, Wei-Shun Yu, and Pei-Chun Lin

***Abstract*—In this study, a hybrid impedance and admittance control strategy is developed as a low-level, high-speed controller for legged robots that fuses two controllers within the range of several ticks of a control loop. This strategy enables the rigid-link legs not only to have accurate motion trajectories but also to adapt to the impacts caused by interactions with unknown environments. In addition, owing to the significantly different characteristics of the leg in compression and in tension, the study introduces a novel switching strategy that adjusts the hybrid level of the controller in the range of the leg stride. The proposed strategy was experimentally validated on a linkage-based leg wheel, and the results confirm the effectiveness of the strategy.**

***Keywords*—Quadruped robot, impedance control, admittance control, leg-wheel, hybrid, switching**

I. INTRODUCTION

The ability to traverse uneven terrains is present in legged robots. Compared to bipedal creatures, quadrupeds have superior stability and adapt more easily to rough terrain. Therefore, quadruped robots are often used to explore unknown environments [1]. With the development of computer science, current mainstream research mainly optimizes the motion trajectory of the body or legs through the high-level controller, enabling the quadruped robot to stably traverse rough terrain [2]. These quadruped robots display good body stability and robustness. However, due to limitations in hardware computational speed, dynamic motion is a challenge for robots. Compared to the stability of body posture, some research focuses more on the effects of leg movements and gait analysis on the dynamic motion of quadruped robots [3]. The spring-loaded inverted pendulum (SLIP) model has been widely verified as a basic movement of the legs [4], and its advantage is that it can describe the complex structure of legged robots through a simplified model, thus simulating the movement trajectory of the biological leg [5-7].

The high-level controller is analogous to the brain of the robot, determining its ideal trajectory in space. Conversely, the lower-level controller acts like the central nervous system in anatomy, controlling the motion performance of the robot's limbs. If the motions of the limbs are not coordinated, even an ideal trajectory will be meaningless. Thus, a well designed lower-level controller is essential for achieving better motion performance in robots. The position PID controller is the most commonly used low-level controller with the best position control error. However, due to its lack of consideration for the impact of the environment, collisions between the robot and the ground can cause a rebound, instigating deviations in the robot's body state [8] and even damaging the mechanism. To track the position command accurately and reduce the impact of the environment, adding passive components to the robot's legs is a common solution [5-7, 9-12], which can be divided into passive and active method. *Passive* method means adding passive components directly to the robot's mechanism, for example, a series elastic actuator (SEA) [9, 11], which is the simplest and most effective method. However, it increases the weight of the robot and the complexity of the system. *Active* means controlling the plant by analogizing it to an impedance system to describe the dynamic relationship between the position and the force of the end effector. This control method is called *impedance control* [13].

Regarding whether the plant is viewed as impedance or admittance, impedance control can be divided into two types [14]. If the plant is viewed as impedance, it is called *impedance control*. Due to its force control implementation, if the plant has unmodeled dynamics, it will result in larger positional errors [8], making it less suitable for robots with high deceleration ratios or more joint friction. [10] implemented impedance control in a low-level controller and achieved a highly dynamic running gait on the MIT Cheetah, benefiting from the motor with only a 1:6 deceleration ratio. If the plant is viewed as admittance, it is called *admittance control* (also termed *position-based impedance control*). The position controller compensates for some of the losses caused by unmodeled dynamics, making it very suitable for robots driven by hydraulic or high-torque motors such as HyQ [12]. Therefore, compared to impedance control, admittance control is more commonly used for legs as a low-level controller of quadruped robots. Its disadvantage is that it lacks more accurate external force estimation. Additionally, the two controllers display different characteristics in response to the rigidity of the environment. When the environment is hard and unyielding, impedance control provides good performance, but when the environment is soft, its accuracy is poor. In contrast, admittance control provides good performance in soft environments but causes contact instability in rigid environments [15]. Therefore, [14] proposed a hybrid control framework to complement the two and demonstrate stability.

Recently, we proposed a novel leg-wheel mechanism [16]. Compared to previous generations of robots in the lab that could only control the deformation and rotation of legs [7], this mechanism can control the end effector's movement on the entire two-dimensional plane. The robot with this new leg wheel not only can quickly pass through flat terrain in wheel mode, but also can make efficient movements in leg mode.

This work is supported by National Science and Technology Council (NSTC), Taiwan, under contract MOST 110-2221-E-002-111-MY3.

The authors are with Department of Mechanical Engineering, National Taiwan University (NTU), No.1 Roosevelt Rd. Sec.4, Taipei 106, Taiwan. (Corresponding email: peichunlin@ntu.edu.tw).

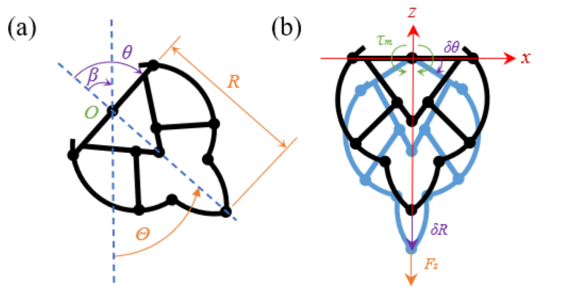

Fig. 1 The leg-wheel module utilized in this work: (a) coordinate definition of the module (b) notations related to the virtual work method.

Previous research [16, 17] found that when using a force controller, friction forces in the transmission system (gear box, belt-and-pulley system, joint friction, etc.) cause a tracking error trajectory. Although position control can improve position accuracy, it will result in larger impacts, rebound in rigid environments, and even damage the mechanism. Therefore, this study applies a hybrid controller to this mechanism to reduce position tracking errors during the swing phase while mitigating the impact during the stance phase. Additionally, the study designed an intuitive and effective control strategy to enhance motion performance during stepping.

The remainder of the paper is organized as follows. In Section II, the coordinate transformation of the leg-wheel module and the estimation of ground reaction force (GRF) through the virtual work method is introduced. Section III presents the hybrid control and proposes a novel control strategy. In Section IV, the effectiveness of the controller and control strategy is verified through single-leg motion experiments. Finally, Section V summarizes the experiments and discusses future work.

II. REVIEW OF THE LEG-WHEEL MODULE

In our previous study [7], we invented a multi-linkage mechanism that can smoothly switch between “wheels” and “leg” and has two degrees of freedom, allowing the end-effector to move in a two-dimensional plane.

A. Coordinate Transformation

Figure 1(a) shows the θ-β coordinate definition of the mechanism. The advantage of this definition is that the length and the angle of the leg are only related to θ and β, respectively. When the module is in wheel mode, $\theta = \theta_0 = 17°$. Since the mechanism is controlled by two motors, we need to convert the motor’s position coordinates (φ_R, φ_L) to the (θ, β) coordinate, which is represented as

$$\begin{bmatrix} \theta \\ \beta \end{bmatrix} = \frac{1}{2}\begin{bmatrix} 1 & -1 \\ 1 & 1 \end{bmatrix}\begin{bmatrix} \varphi_R \\ \varphi_L \end{bmatrix} + \begin{bmatrix} 1 \\ 0 \end{bmatrix}\theta_0 \tag{1}$$

In this study, the leg-wheel module was modeled as a virtual linear spring-damper system and a torsional spring-damper system. For convenience, we converted the (θ, β) coordinate into polar coordinates and represented the length and angle of the leg as (R, Θ), respectively. However, the relationship between the θ and the change in leg length R is nonlinear, which involves the complex kinematics of the mechanism. This study used first-order approximation to improve the computing efficiency. The relationship between the (θ, β) coordinate and the (R, Θ) coordinate can be represented as

$$\begin{bmatrix} R \\ \Theta \end{bmatrix} \approx \begin{bmatrix} \gamma\theta + b \\ -\beta \end{bmatrix}$$
$$\text{where} \begin{cases} \gamma = \dfrac{dR}{d\theta} = 103.7217 \text{ mm/rad} \\ b = 66.6731 \text{ mm} \end{cases} \tag{2}$$

B. Ground Reaction Force Estimation

In the design of the controller, the external force applied to the module needs to be taken as the controller’s input. Due to the complicated forward kinematics of the module [16], developing its dynamic model using the variables θ and β is challenging. Hence, in [7], the virtual work approach is utilized, which calculates the relationship between the motor’s applied torque and GRF using static balance. In this method, only a point mass located at the hip (point O) is taken into account, and the linkages are treated as weightless. Figure 1(b) illustrates the notation associated with the virtual work derivation. The virtual work of the leg-wheel is expressed as follows:

$$F_Z = 2\tau_m \frac{\delta\theta}{\delta R} \approx \frac{2}{\gamma}\tau_m \tag{3}$$

Conversely, to convert the end-effector’s force command into the motor’s torque input, the following equation can be obtained by rearranging

$$\tau_m = \frac{F_Z}{2} \cdot \frac{\delta R}{\delta\theta} \approx \frac{\gamma}{2}F_Z \tag{4}$$

III. CONTROLLER FRAMEWORK

Controlling the interaction between the end-effector and the ground is vital for reducing the impact caused by unknown environments during the motion of the foot. Impedance control is a form of indirect force control that integrates the characteristics of virtual passive elements into the rigid mechanical structure, enabling it to comply with the effects of the external environment during motion. The controller can be divided into impedance control and admittance control based on the input of the displacement or external force caused by the external environment. Although both control frameworks are aimed at analogizing the original system into a virtual mass-spring-damper system, the causal relationship between force and displacement makes the two controllers more suitable for different scenarios. This section will provide a detailed explanation of the hybrid control and a strategy designed for quadruped robots based on their actual walking conditions.

A. Impedance Controller

In impedance control, the plant acts as a mechanical impedance, and the environment serves as admittance. In other words, the plant perceives the motion input from the external environment and produces force output based on the impedance of simulated passive elements or virtual touch

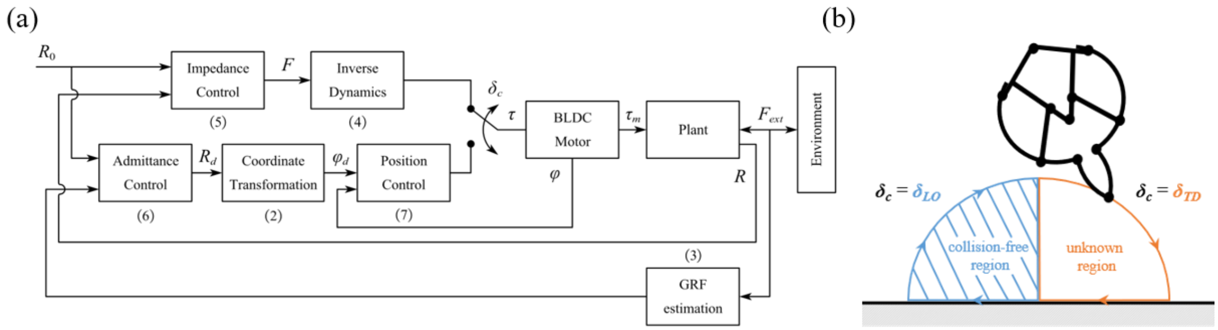

Fig. 2 The overall controller used for the leg-wheel module. (a) shows the implementation of hybrid control, and (b) shows the stepping control strategy.

objects. Given that the proportion of the mass of the foot mechanism relative to the mass of the quadruped robot is very small, a common assumption is to ignore the mass of the foot mechanism to simplify the motion model of the entire robot, which is a common assumption in past research [18].

Therefore, if the plant is modeled as a virtual spring-damping system, the relationship between displacement and external force caused by the environment can be written using the following equation:

$$F = D\left(\dot{R} - \dot{R}_0\right) + K(R - R_0) \tag{5}$$

where F represents the control force, R represents the actual leg length, R_0 represents the leg length at equilibrium, K represents the spring constant, and D represents the damping constant. Finally, the control force F can be converted into a motor torque command $\tau_{impedance}$ by (4).

B. Admittance Controller

In contrast to impedance control, admittance control considers the external environment as the impedance (i.e., mass-spring-damper system), and the plant acts as the admittance, complying with the external forces caused by the environment.

The position change of the plant in relation to the estimated external force by the GRF estimator can be represented by the following equation:

$$D\left(\dot{R}_0 - \dot{R}_d\right) + K(R_0 - R_d) = F_{ext} \tag{6}$$

where F_{ext} represents the external force, R_d represents the ideal length of the foot, R_0 represents the length at equilibrium, K represents the spring constant, D represents the damping constant. The solution of R_d serves as the input to the plant.

To implement admittance control, a position controller is needed since it uses position changes as input. For quadruped robots, reducing steady-state errors is not as important as having dynamic behavior. Therefore, a PD controller was adopted for position control, with the foot length R_d into the ideal position φ_d using (2), as the motor command represents

$$\tau_{admittance} = K_d\left(\dot{\varphi} - \dot{\varphi}_d\right) + K_p(\varphi - \varphi_d) \tag{7}$$

where φ is the actual motor position, φ_d is the desired motor position, K_p and K_d are the control parameters of the PD controller.

C. Hybrid Controller

In theory, the two different control strategies are equivalent when the control frequency is infinitely large; however, this is not possible in practical applications. Therefore, although their goals are the same, the two control strategies still have different characteristics in practical applications due to the different causal relationships between force and displacement. When the environment is stiff, impedance control provides very good performance, but it cannot compensate for the effects of un-modeled dynamics (e.g., friction force), and it lacks accuracy. On the other hand, admittance control is an ideal choice for soft environments. Position control can compensate for the errors caused by unmodeled dynamics, but the input delay of the system worsens its performance in stiff environments and may even cause contact instability [15].

To further improve the performance of the two controllers, a hybrid control architecture is proposed in [14], which switches between the two controllers during a certain time duration to achieve complementary effects and prove stability. The switching of controllers can be represented as

$$\tau = \begin{cases} \tau_{impedance}, & \dfrac{\mathrm{mod}(t,\ T_c)}{T_c} \leqslant \delta_c \\ \tau_{admittance}, & \dfrac{\mathrm{mod}(t,\ T_c)}{T_c} > \delta_c \end{cases} \tag{8}$$

where τ represents the torque input of the plant, $\tau_{impedance}$ and $\tau_{admittance}$ represent the torque input calculated by the impedance controller and the admittance controller respect-tively, T_c represents the duration of controller switching, δ_c represents the duty cycle of the controller switching, and mod (number, divisor) function returns the remainder after a number is divided by a divisor. The system can be more inclined to the characteristics of a single controller by changing the size of δ_c to adjust the proportion between the impedance controller and the admittance controller. Through this control architecture, we can adjust according to the needs of different situations. Figure 2(a) shows the implementation of hybrid control.

D. Stepping Control Strategy

In previous studies [16, 17], we found that when controlling the position of the end-effector using a position controller, although a smaller tracking error occurs during the swing phase, the end of the foot is not equipped with an extra force sensor to determine whether the end-effector is touching the ground.

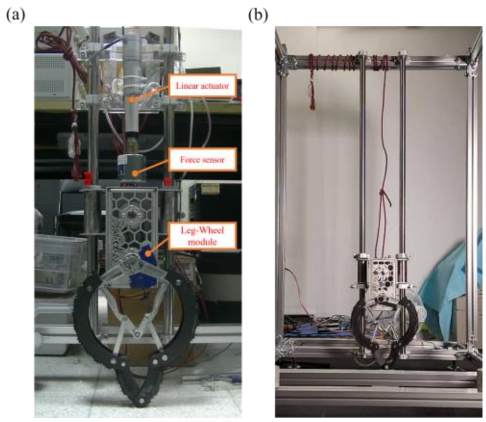

Fig. 3 Experimental platform for (a) virtual stiffness estimation, and (b) dynamic jumping and continuous stepping.

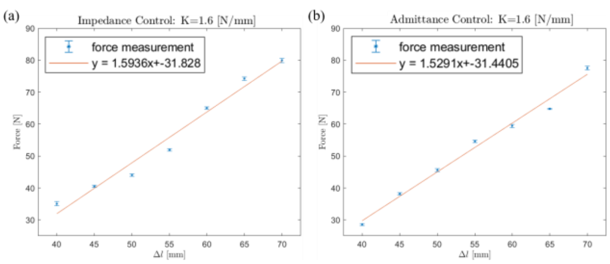

Fig. 4 Stiffness estimation using (a) impedance and (b) admittance control.

This causes the foot to move the instant it enters the stance phase, and the mechanism is unable to absorb the impact within a short timeframe, causing the end-effector to generate an impulse force, resulting in end-effector bounce or even causing damage to the mechanism. However, when controlling through a force controller, although it can effectively reduce the impact on the mechanism, the friction forces in the transmission system (gearbox, belt-and-pulley system, joint friction, etc.) cause a large tracking error. Even the static friction forces cannot be overcome.

In addition, a novel control strategy is proposed in this paper. As shown in Figure 2(b), the whole single-stepped motion cycle is divided into two stages, namely, Touch Down (TD) and Lift Off (LO). During TD, we tend to use the impedance controller, as it interacts with the rigid environment better. During LO, we tend to use the admittance controller, as it has a smaller tracking error in the collision-free region, and the PD controller within can better compensate for the impact of friction force. As shown in Figure 2(b), we denote δ_c during TD as δ_{TD} and during LO as δ_{LO}, and set δ_c as

$$\delta_c = \begin{cases} \delta_{TD}, & \dfrac{\operatorname{mod}(t,\ T_{step})}{T_{step}} \leqslant 0.5 \\ \delta_{LO}, & \dfrac{\operatorname{mod}(t,\ T_{step})}{T_{step}} > 0.5 \end{cases} \tag{9}$$

To improve the single-stepped motion performance, where T_{step} represents the period of a single step and mod (number, divisor) function returns the remainder after a number is divided by a divisor.

IV. Experiment

In this section, we evaluated the effectiveness of the impedance control and the admittance control applied to the wheel-leg module through static compression and dynamic jumping experiments to showcase the characteristics of the spring-damping system. Furthermore, we verified through the continuous-stepping experiment whether switching between the two controllers can improve the performance of the quadruped during continuous stepping movements.

A. Experimental Setup

Figure 3(a) shows the leg-wheel module and platform used in the experiment. The leg-wheel module weighs 0.7 kg, and the motor module weighs 4.3 kg. The motor module is driven by two brushless DC motors (HT-04, Haitai Inc.) with a gear ratio of 1:6, which drives the two degrees of freedom of the leg-wheel mechanism through a belt-and-pulley system. The built-in driver boards (STM32F446RE) are used for the position control loop and current control, and the control frequency is 40 kHz. The controller and GRF estimator were programmed using LabView and utilized using a real-time embedded controller (sbRIO9629, National Instruments) by sending the desired position and desired current command through CAN Bus at 500 Hz.

B. Virtual Stiffness Estimation Experiment

In this experiment, the leg-wheel module was controlled by both impedance control and admittance control individually, simulating a virtual spring with stiffness. Figure 3(a) shows the experimental platform, where the leg-wheel module was connected to a sliding joint consisting of two rails on the frame for vertical movement. A linear actuator is fixed on the rail to measure the compression length. The linear actuator is connected to a force sensor that records the external force during compression.

Figure 4 shows the results obtained by compressing the leg-wheel module with stiffness K = 1.6 N/mm and initial length R_0 = 320 mm. The stiffness measured by each controller was 1.5936 N/mm and 1.5291 N/mm, respectively, which were close to the set stiffness.

C. Dynamic Jumping Experiment

In this experiment, we will simulate the leg-wheel module as a spring-damper system through impedance control and admittance control. Figure 3(b) shows the vertical motion platform for this experiment, which allows the module to perform a vertical motion on the slider joint. The steps of the experiment are as follows: first, we used two different controllers to simulate the leg-wheel module as a virtual spring-damper system with stiffness K = 1.6 N/mm, damping D = 0.02 N/mm^2, and initial length R_0 = 320 mm. The module was then compressed to 150 mm and released. The motion of the module was captured by VICON and compared with the 1-DOF TD-SLIP model [19].

Figure 6 shows the trajectory after LO. As observed, the impedance controller has a faster response time; however, the jumping height of the module is significantly different from the ideal jumping height because of friction in the slider joint, and the impedance control cannot compensate for the friction loss caused during the LO process through force control. When the

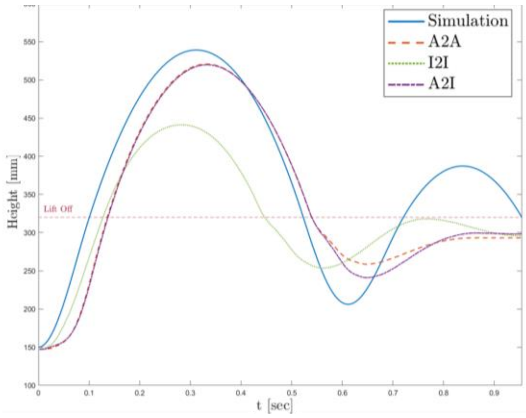

Fig. 6 Jumping trajectory using different controller. (Note: In the legend, A2A represents admittance to admittance, I2I represents impedance to impedance, and A2I represents admittance to impedance.)

controller was set to admittance control, the position control compensated for the part of friction loss during the jump. Thus, the jumping height of the module was close to the theoretical height. However, a delay in the jumping trajectory and a larger discrepancy between the amount of compression at the landing and the theoretical value were observed, which are attributed to the following reasons:

- The admittance controller uses the external force on the system as the controller input; thus, the lower the control frequency of the GRF estimator, the more obvious the delay phenomenon becomes.
- The GRF estimator was realized by a virtual work method, which does not consider the mass and acceleration of each linkage in the mechanism. As a result, there was a discrepancy between the external force calculated by the virtual work method and the actual external force experienced by the system during dynamic motion.

D. Continuous Stepping Experiment

In this experiment, we combined the hybrid controller and the stepping control strategy to improve the performance during single-leg movement. It is difficult to Set up the experimental platform for the 2-DOF motion of the leg. Therefore, in this study, 1-DOF vertical motion is used to simulate the stepping motion (i.e., the angle of the foot Θ was set to 0 throughout the motion).

Figure 3(b) shows the experimental platform, which was the same as the dynamic jumping experiment. The only difference was that the lower limit of the module's position was restricted. When the module was in the swing phase, the height was maintained. When the module was in the swing phase, the height remained fixed to simulate the body posture of the walking gait. When in the stance phase, it is lifted with the leg extension to simulate the posture change of the body.

In this experiment, the leg-wheel module served as a virtual spring-damper system with stiffness K= 1.6 N/mm and damping D = 0.02 N/mm^2, and set the equilibrium length R0 of the foot to be a sinusoidal wave with a frequency of 1.5 Hz ranging from 150 mm to 320 mm, as per the command. For the hybrid controller, we set the time duration to four control loop

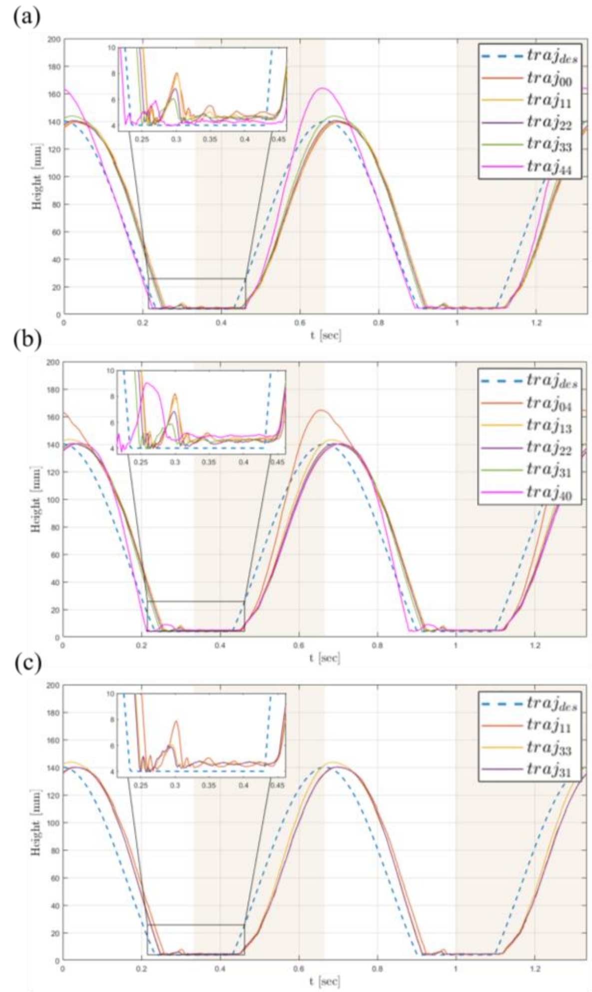

Fig. 5 Motion trajectory of the end-effector during two stable cycles using (a) hybrid controller only, (b) hybrid controller with the stepping control strategy, and (c) compared the results of the two. (Note: In the legend, the first subscript digit represents δ_{TD}, and the second represents δ_{LO}. The number 0, 1, 2, 3, 4 represents δ_c = 0, 0.25, 0.5, 0.75, 1.

counts (i.e., T_c = 4 * 0.002 s = 0.008 s) and the duty cycle δ_c = 0, 0.25, 0.5, 0.75, 1. δ_c = 0 represents pure admittance control, while δ_c = 1 represents pure impedance control.

1) Using hybrid controller only: Figure 5(a) shows the steady-state motion trajectory of the end-effector during continuous stepping. The experimental results of the swing phase and stance phase will be discussed separately.

a) In the swing phase: The experimental results showed that as δc approaches 0 (i.e., the controller is closer to a pure admittance controller), the end-effector gets closer to the ideal trajectory, but the delay phenomenon becomes more obvious. The cause of this phenomenon is the low control frequency of the GRF estimator. When the duty cycle approaches 1, the delay phenomenon disappears. Compared to the GRF estimator's 500 Hz, the motor's encoder control frequency is 40 kHz, which can effectively reduce the impact of input delay. However, at the same time, the measured trajectory amplitude is much larger than the ideal trajectory. The reason is that in the analog process of the leg-wheel module to the spring-damper, it is assumed that the leg has no mass. However, in reality, the leg has a mass of 0.7 kg, which makes the whole system underdamped with a damping ratio $\zeta = 0.01$, thereby causing resonance in the system.

b) In the stance phase: The experimental results showed that as δ_c approaches 0 (i.e., the controller is closer to a pure admittance controller), the end-effector produces a larger rebound distance that gradually decreases as δ_c approaches 1 until the controller becomes a pure impedance controller. Although a bounce-back still occurs when $\delta_c = 1$, the rebound distance is the minimum without multiple rebounds.

2) Using hybrid controller with the stepping control strategy: Finally, we expected to improve the performance during continuous stepping using the Stepping Control Strategy. Figure 5(b) shows the experimental results under different switching strategies. Surprisingly, the maximum rebound height is obtained when $\delta_{TD} = 1$ and $\delta_{LO} = 0$ (i.e., pure impedance controller to pure admittance controller) due to the discontinuity of the two controllers during switching. As mentioned in Section C.1, the impedance controller is more susceptible to the effects of unmodeled dynamics. The discontinuity of the trajectory during the swing phase can be observed clearly from $\delta_{TD} = 0$ and $\delta_{LO} = 1$. The results from Figure 5(b) also show that this control strategy has the best performance among all trajectories when $\delta_{TD} = 0.75$ and $\delta_{LO} = 0.25$. Although the delay phenomenon still exists, it meets the criteria of having a similar height to the reference trajectory in the swing phase and the minimum rebound height upon landing. Moreover, since both the TD and LO phases are a mixture of impedance and admittance controllers, no discontinuous trajectory phenomenon appears. Figure 5(c) further illustrates that compared with using only the hybrid controller, this control strategy combines the characteristics of both types of trajectories with a smaller rebound height and better positional tracking error, thus proving the effectiveness of this control strategy.

V. Conclusion and Future Work

In this study, a control strategy that hybridizes impedance control and admittance control was developed as a lower-level and high-speed controller within the range of several ticks of the control loop. This enables the leg-wheel composed of rigid linkages to act as a spring-damping system. Thus, the leg-wheel can reduce its ground impact during landing, and it has a smaller tracking error during the aerial phase. Additionally, a novel switching strategy in the range of the leg stride was proposed. The experimental results illustrate that the hybrid use of impedance and admittance control with different ratios during the stance and aerial phases can yield the best response.

The fusion of impedance control reduces the impact of input delay and the inaccuracies of force estimation caused by the admittance control and GRF estimator during dynamic motion respectively. Nonetheless, there is still a discrepancy between the actual performance and the ideal trajectory. In the future, the external force estimator based on multi-body dynamics proposed in previous research [17] will be used as a GRF estimator to enhance the performance of the motion under this control architecture.

Reference

[1] M. Vukobratovic, Dynamics and robust control of robot-environment interaction. World Scientific, 2009.

[2] D. Kim, J. Di Carlo, B. Katz, G. Bledt, and S. Kim, "Highly dynamic quadruped locomotion via whole-body impulse control and model predictive control," arXiv preprint arXiv:1909.06586, 2019.

[3] R. J. Full and D. E. Koditschek, "Templates and anchors: neuromechanical hypotheses of legged locomotion on land," Journal of experimental biology, vol. 202, no. 23, pp. 3325-3332, 1999.

[4] R. Blickhan, "The spring-mass model for running and hopping," Journal of biomechanics, vol. 22, no. 11-12, pp. 1217-1227, 1989.

[5] J. K. Yim, E. K. Wang, and R. S. Fearing, "Drift-free roll and pitch estimation for high-acceleration hopping," in 2019 International Conference on Robotics and Automation (ICRA), 2019: IEEE, pp. 8986-8992.

[6] D. Lakatos et al., "Dynamic locomotion gaits of a compliantly actuated quadruped with slip-like articulated legs embodied in the mechanical design," IEEE Robotics and Automation Letters, vol. 3, no. 4, pp. 3908-3915, 2018.

[7] W.-H. Chen, H.-S. Lin, Y.-M. Lin, and P.-C. Lin, "TurboQuad: A novel leg–wheel transformable robot with smooth and fast behavioral transitions," IEEE Transactions on Robotics, vol. 33, no. 5, pp. 1025-1040, 2017.

[8] J.-H. Kim et al., "Legged robot state estimation with dynamic contact event information," IEEE Robotics and Automation Letters, vol. 6, no. 4, pp. 6733-6740, 2021.

[9] P. Fankhauser and M. Hutter, "Anymal: a unique quadruped robot conquering harsh environments," Research Features, no. 126, pp. 54-57, 2018.

[10] D. J. Hyun, S. Seok, J. Lee, and S. Kim, "High speed trot-running: Implementation of a hierarchical controller using proprioceptive impedance control on the MIT Cheetah," The International Journal of Robotics Research, vol. 33, no. 11, pp. 1417-1445, 2014.

[11] M. Hutter, C. Gehring, M. Bloesch, M. A. Hoepflinger, C. D. Remy, and R. Siegwart, "StarlETH: A compliant quadrupedal robot for fast, efficient, and versatile locomotion," in Adaptive Mobile Robotics: World Scientific, 2012, pp. 483-490.

[12] C. Semini et al., "Towards versatile legged robots through active impedance control," The International Journal of Robotics Research, vol. 34, no. 7, pp. 1003-1020, 2015, doi: 10.1177/0278364915578839.

[13] N. Hogan, "Impedance control: An approach to manipulation," in 1984 American control conference, 1984: IEEE, pp. 304-313.

[14] C. Ott, R. Mukherjee, and Y. Nakamura, "A Hybrid System Framework for Unified Impedance and Admittance Control," Journal of Intelligent & Robotic Systems, vol. 78, no. 3-4, pp. 359-375, 2014, doi: 10.1007/s10846-014-0082-1.

[15] T. Valency and M. Zacksenhouse, "Accuracy/robustness dilemma in impedance control," J. Dyn. Sys., Meas., Control, vol. 125, no. 3, pp. 310-319, 2003.

[16] H.-Y. Chen, T.-H. Wang, K.-C. Ho, C.-Y. Ko, P.-C. Lin, and P.-C. Lin, "Development of a novel leg-wheel module with fast transformation and leaping capability," Mechanism and Machine Theory, vol. 163, 2021, doi: 10.1016/j.mechmachtheory.2021.104348.

[17] Y.-J. Liu and P.-C. Lin, "Development of a dynamic model of the 11-linkage and closed-chain leg-wheel module," in 2022 IEEE/ASME International Conference on Advanced Intelligent Mechatronics (AIM), 2022: IEEE, pp. 1082-1088.

[18] L.-J. Chen and P.-C. Lin, "Gait Pattern Stabilization using Central Pattern Generator with Foothold Force Optimization for Quadruped Robots," in 2022 IEEE/ASME International Conference on Advanced Intelligent Mechatronics (AIM), 2022: IEEE, pp. 1658-1663.

[19] J. Jae Yun and J. E. Clark, "Dynamic stability of variable stiffness running," presented at the 2009 IEEE International Conference on Robotics and Automation, 2009.